ketone, 6004-59-7; cyclohexylmethyl cyclohexanecarboxylate, 2611-02-1; cyclohexanecarboxaldehyde, 2043-61-0; hydroxymethylcyclohexane, 100-49-2; cyclohexyl *p*-tolyl ketone, 2789-44-8; cyclohexyl *m*-tolyl ketone, 3277-78-9; cyclohexyl *o*-tolyl ketone, 2936-55-2; cyclohexyl 2-thienyl ketone, 79852-25-8; cyclohexyl 3-thienyl ketone, 36646-69-2; cyclohexyl 2-furyl ketone, 111609-50-8; cyclohexyl 3-furyl ketone, 36646-68-1; cyclohexyl 2-pyrrolyl ketone, 75211-59-5; 2-thiophenecarboxaldehyde, 98-03-3; 3-thiophenecarboxaldehyde, 498-62-4; 2-furancarboxaldehyde, 98-01-1; 3-furancarboxaldehyde, 498-60-2; 2-pyrrolecarboxaldehyde, 1003-29-8; cyclohexene, 110-83-8; cyclopentene, 142-29-0; cyclooctene, 931-88-4.

Electrochemical Oxidation of Xanthosine. Isolation and Structure Elucidation of a New Dimeric Xanthine Nucleoside

Xinhua Ji, P. Subramanian, Dick van der Helm, and Glenn Dryhurst*

Department of Chemistry and Biochemistry, University of Oklahoma, Norman, Oklahoma 73019

Received July 13, 1989

Electrochemical oxidation of xanthosine (**2**) at pH 2 at a pyrolytic graphite electrode generates an electrophilic radical cation intermediate. Nucleophilic attack by **2** on this radical results, ultimately, in formation of 3-(8-xanthosyl)xanthosine (**7**). Hydrolytic cleavage of one ribose residue from **7** in acidic solution leads to 3-(8-xanthosyl)xanthine (**8**). The structure of **8**, a new dimeric xanthine nucleoside, has been established using spectral and X-ray diffraction methods.

Ultraviolet irradiation of adenosine, guanosine, and xanthosine in the presence of the corresponding 8-bromopurine ribonucleoside yields (8 → 8) coupled biribonucleosides.[1,2] Thus, photolysis of an equimolar mixture of 8-bromoxanthosine and xanthosine in aqueous solution gives 8-(8-xanthosyl)xanthosine (**1**) in very low yield. Similarly, photolysis of a mixture of, for example, 8-bromoadenosine and xanthosine yields 8-(8-xanthosyl)-adenosine.

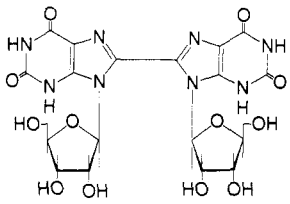

1

Recently, we reported that electrochemical oxidation of near-saturated solutions of xanthosine (ca. 2 mM) at pH 2 resulted in a rather complex mixture of products.[3,4] One major oxidation product was an unstable dimer of xanthosine, which readily lost one ribose unit to yield a compound which, apparently, consisted of one xanthosine residue and one xanthine residue. The UV absorption spectra of these electrochemically synthesized dimers are quite different from that of photodimer **1**, thus suggesting that a method had been discovered to synthesize a new class of dimeric nucleosides. Based upon our earlier results we were not able to elucidate the exact molecular structures of the electrochemically generated xanthosine dimers.

In this report the electrochemical synthesis and isolation of a new (xanthosyl)xanthine dimer is described along with spectral and X-ray diffraction information which permits the unequivocal establishment of its unusual molecular structure. We also propose a mechanism for the electrode process which leads to this and other reaction products.

Experimental Section

Xanthosine dihydrate was obtained from Sigma (St. Louis, MO) and was used without further purification. Conventional equipment was used for electrochemical studies.[5] A pyrolytic graphite electrode (Pfizer Minerals, Pigments and Metals Division, Easton, PA) having an approximate surface area of 4 mm^2 was used for voltammetry. Controlled-potential electrolyses employed two plates of pyrolytic graphite (ca. 30 cm^2 surface area) and a conventional three-compartment cell containing a platinum gauze counter electrode and a saturated calomel reference electrode (SCE). All potentials are referred to the SCE at ambient temperature. Electrolyses were carried out in pH 2.0 phosphate buffer having an ionic strength of 0.5.[6] Typically, an excess of xanthosine was vigorously stirred in the latter buffer solution for about 1 h. Thirty milliliters of this solution was then filtered, and the filtrate (i.e., saturated xanthosine) was transferred into the working electrode compartment of the electrochemical cell. Phosphate buffer at pH 2.0 was used in the counter electrode compartment. The solution in the working electrode compartment was stirred with a Teflon-coated magnetic stirring bar, and nitrogen gas was bubbled vigorously through the solution. The electrolysis was performed at a constant potential of 1.07 V. Typically, the electrolysis was allowed to proceed for 30–40 min, and then 2 mL of the solution was removed for separation by high-performance liquid chromatography (HPLC). Without stopping the electrolysis 2 mL of a saturated solution of xanthosine in pH 2.0 phosphate buffer, which also contained some undissolved compound, was added to the working electrode compartment. The electrolysis was then continued for another 40 min (the time required for one complete HPLC separation), and the entire sequence was repeated.

HPLC was carried out with a Bio-Rad Model 1300 pump, a Rheodyne Model 7125 loop injection (2.0-mL loop) and a Gilson Holochrome UV Detector (254 nm). A reversed-phase column (Brownlee Laboratories; RP-18, 5 μm, 25 × 0.7 cm) and a short guard column (Brownlee Laboratories, RP-18, 5 μm, OD-GU, 5 × 0.5 cm) were used for all HPLC separations. An isocratic separation method was employed with 0.1 M formic acid in water adjusted to pH 4.0 with concentrated ammonium hydroxide as the mobile phase. The flow rate was 4 mL min^{-1}. Compound **8** eluted under chromatographic peak E (Figure 2) and was

(1) Bose, S. N.; Davies, R. J. H.; Anderson, D. W.; van Niekerk, J. C.; Nassimbeni, L. R.; Macfarlane, R. D. *Nature (London)* **1978**, *271*, 783–784.
(2) Joshi, P. C.; Davies, R. J. H. *J. Chem. Res. S.* **1981**, 2701–2732.
(3) Tyagi, S. K.; Dryhurst, G. *J. Electroanal. Chem. Interfacial Electrochem.* **1987**, *216*, 137–156.
(4) Subramanian, P.; Tyagi, S. K.; Dryhurst, G. *Nucleosides Nucleotides* **1987**, *6*, 25–42.
(5) Owens, J. L.; Marsh, H. A.; Dryhurst, G. *J. Electroanal. Chem. Interfacial Electrochem.* **1978**, *91*, 231–247.
(6) Christian, G. D.; Purdy, W. C. *J. Electroanal. Chem. Interfacial Electrochem.* **1962**, *3*, 363–367.

0022-3263/90/1955-1291$02.50/0 © 1990 American Chemical Society

collected in a flask maintained at −80 °C in dry ice. Repetitive 2-mL injections of the electrolyzed solutions were made in order to collect a few milligrams of 8. The resulting frozen solution was melted only immediately before the desalting step. This was accomplished by an HPLC method using the same reversed-phase column but the mobile phase was water adjusted to pH 3.0 with trifluoroacetic acid; the flow rate was 4 mL min^{-1}. Two-milliliter injections of 8 dissolved in pH 4.0 ammonium formate solution were made. Ammonium formate eluted rapidly from the column. Compound 8 eluted with a retention time of 18 min. The eluent containing 8 was collected in a freeze-drying flask maintained at −80 °C and was freeze-dried to give a white fluffy solid.

Fast atom bombardment–mass spectrometry (FAB-MS) was performed with a VG Instruments Model ZAB-E spectrometer. ^1H NMR spectra were recorded on a Varian Model XL-300 (300 MHz) spectrometer. UV spectra were recorded on a Hitachi 100-80 spectrophotometer.

X-ray Crystallography. The freeze-dried sample of 8 was dissolved in deionized water at 40 °C, and then the temperature was gradually lowered to 4 °C. The sample was stored at 4 °C for 30 days during which time very slow evaporation of water occurred and small, thin, boat-shaped crystals were formed. A crystal having dimensions of 0.03 × 0.10 × 0.33 mm was used for the space group determination and data collection on an Enraf-Nonius CAD-4 diffractometer using Ni-filtered Cu Kα radiation [λ(Cu K$\bar{\alpha}$) = 1.541 78 Å and μ = 11.43 cm^{-1}] at −110 (1) °C. No systematic absences were observed and the space group should be $P\bar{1}$ dictated by the chiral atom C(1′) in the molecule (see Figure 3). Forty-eight reflections ($29° > \theta > 15°$) and Cu Kα_1 wavelength (1.540 51 Å) were used for lattice constances: a = 9.596 (2), b = 11.236 (2), and c = 8.504 (1) Å; α = 96.09 (2), β = 108.00 (2), and γ = 107.18 (2)°; and V = 813.2 Å^3. Z = 2 for $C_{15}H_{14}N_8O_8$ (FW = 434.33), and D_{calc} = 1.77 g/cm^3; 3883 data within $0 \le h \le 12$, $-14 \le k \le 14$ and $-10 \le l \le 10$ were collected using $\omega - 2\theta$ scan techniques and a variable scan width calculated as (1.10 + 0.20 tan θ)°. The maximum scan time for a single reflection was 120 s. The receiving aperture, located 173 mm from the data crystal, had a constant height of 6 mm and a variable width calculated as (4.50 + 0.43 tan θ) mm. Three orientation control monitors were measured every 7200 s of X-ray exposure time, showing a maximum difference of 0.025 and an esd of 0.005. The profiles of all the measured reflections were observed and stored.

The data set was processed by using a profile analysis method.[7] Lorentz-polarization corrections were applied. No absorption correction was made. Among 3560 unique data, there were 3143 observed ones [$I \ge 2\sigma(I)$]. The structure was solved by the direct method using the program MITHRIL.[8] Instead of using the phase permutation technique, the random phases for 300 unknown phases ($E \ge 1.548$) were used in the starting set and refined with the tangent formula. The theory of this technique has been discussed by Yao.[9] Although the space group should be noncentrosymmetric, as mentioned above, the statistics of the data analysis indicated that the structure had partial centrosymmetric features. Following several failures of running the MITHRIL with respect to the space group $P\bar{1}$, a test run with $P\bar{1}$ was carried out, resulting in a partial structure of one molecule consisting of 24 non-hydrogen atoms. This partial structure was then refined in the space group $P\bar{1}$, and the whole structure of two separate molecules was completed from successive difference Fourier syntheses, by using SHELX76.[10] All the non-hydrogen atoms were refined anisotropically. The locations of all 28 hydrogen atoms were determined from successive difference Fourier syntheses and refined isotropically except for fixed temperature factors for H(1′)A, H(O2′)A, H(1′)B, H(3′)B, and H(4′)B. A final R of 0.041 and R_w of 0.047 were obtained by the blocked-matrix least-squares minimization of $\sum_w(|F_o| - |kF_c|)^2$, where $w = 1/[\sigma^2(F) + 0.000600F^2]$. The maximum shift/sd = 0.067 for non-hydrogen atoms and 0.030 for hydrogen atoms in the final refinement. The largest and the smallest peaks in the final difference Fourier map were +0.26 and −0.33 e/Å^3. The error of fit = $[\sum w(F_o - F_c)^2/(N - NP)]^{1/2}$ was 1.30, where N is the number of data used (3143) and NP is the number of parameters refined (664). The final fractional coordinates and isotropic equivalent temperature factors for non-hydrogen atoms are given in Table I.

(7) Blessing, R. H. *Cryst. Rev.* **1987**, *1*, 3–58.
(8) Gilmore, C. J. MITHRIL, *Program for Automatic Solution of Crystal Structures from X-Ray Data*; University of Glasgow Printing Department: Glasgow, Scotland, 1983.
(9) Yao, J.-X. *Acta Crystallogr.* **1981**, *A37*, 642–644; **1983**, *A39*, 35–37.
(10) Sheldrick, G. M. SHELX76, *Program for Crystal Structure Determination*; University of Cambridge: England, 1976.

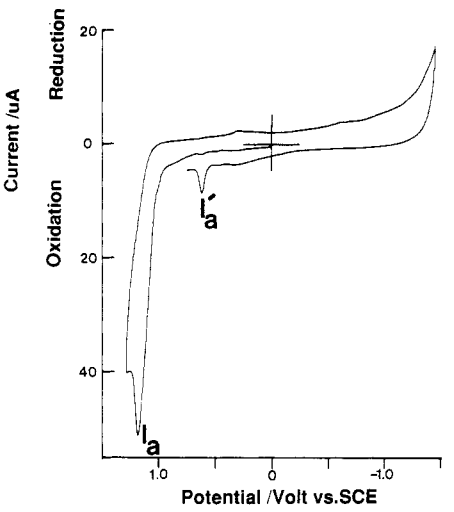

Figure 1. Cyclic voltammograms at the PGE of 2 mM xanthosine in pH 2.0 phosphate buffer (μ = 0.5). Sweep rate: 200 mV s^{-1}.

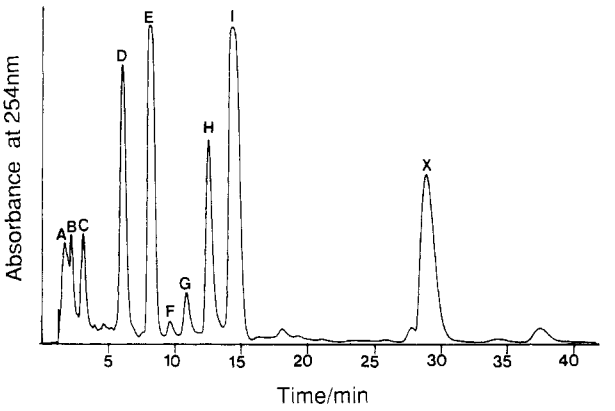

Figure 2. Chromatogram of the product solution formed upon controlled potential electrolysis of a saturated solution of xanthosine in pH 2.0 phosphate buffer (μ = 0.5) for 90 min at 1.07 V. Injection volume: 2.0 mL. Chromatographic conditions are given in the Experimental Section.

3-(8-Xanthosyl)xanthine (8). Compound 8 was isolated as a white, fluffy solid. In aqueous solution 8 showed the following spectra, λ_{max} ($\epsilon_{max} \times 10^{-3}$, L mol^{-1} cm^{-1}): 264 nm (13.3), 235 nm (sh 6.0) at pH 1.0; 265 nm (14.6) at pH 7.0; 276 nm (12.8), 255 nm (sh 9.3) at pH 13.0. FAB-MS (thioerythritol/thiothreitol matrix) m/e (relative abundance); 435 (MH^+, 86), 303 (44, $MH^+ - C_5H_8O_4$), 275 (6.2, $MH^+ - [C_5H_8O_4 + CO]$), 259 (2.5), 152 (27, $C_5H_4N_4O^{\bullet}_2{}^+$, i.e., xanthine); accurate mass measurements on MH^+ gave m/e 435.0991 ($C_{15}H_{15}N_8O_8$) calcd m/e = 435.1015; ^1H NMR (Me_3SO-d_6) δ 11.48 (s, 1 H, N-H), 11.39 (s, 1 H, N-H), 10.79 (s, 2 H, 2 N-H), 7.97 (s, 1 H, C(8)-H), 5.43 (d, J = 6.9 Hz, 1 H, C(1′)-H), 5.09 (m, 1 H, C(2′)-H), 4.20 (m, 1 H, C(3′)-H), 4.02 (m, 1 H, C(4′)-H), 3.72 (m, 2 H, C(5′)-H).

Results

A cyclic voltammogram of xanthosine (2) in pH 2.0 phosphate buffer (Figure 1) shows one well-defined oxidation peak (I_a). After scan reversal several poorly resolved reduction peaks appear, the most noticeable bearing at ca. 0.4 and −0.6 V. On the second anodic sweep a new oxidation peak (I_a') appears at 0.63 V. The peak potential (E_p) for peak I_a measured at pH 2.0 at a slow sweep rate (5 mV s^{-1}) and high concentration (2 mM) of 2 is 1.18 V.

Table I. Final Coordinates and Isotropic Equivalent Thermal Parameters (U_{eq}) for Non-hydrogen Atoms with esd's in Parentheses

$U_{eq} = \frac{1}{3}\sum\sum U_{ij}a^*_i a^*_j \mathbf{a}_i \cdot \mathbf{a}_j$ (Å^2)

atom	x	y	z	U_{eq}
N(1)A	0.07980 (0)	0.35720 (0)	0.47455 (0)	0.020 (1)
C(2)A	0.2009 (5)	0.4733 (4)	0.5276 (4)	0.020 (1)
O(2)A	0.1805 (3)	0.5725 (3)	0.4962 (4)	0.024 (1)
N(3)A	0.3456 (4)	0.4726 (3)	0.6173 (4)	0.016 (1)
C(4)A	0.3638 (4)	0.3583 (4)	0.6356 (4)	0.018 (1)
C(5)A	0.2465 (5)	0.2424 (4)	0.5777 (5)	0.018 (1)
C(6)A	0.0864 (5)	0.2363 (4)	0.4973 (5)	0.018 (1)
O(6)A	−0.0324 (3)	0.1433 (3)	0.4482 (4)	0.023 (1)
N(7)A	0.3064 (4)	0.1456 (3)	0.6100 (4)	0.018 (1)
C(8)A	0.4549 (4)	0.2047 (4)	0.6860 (4)	0.017 (1)
N(9)A	0.4999 (4)	0.3370 (3)	0.7106 (4)	0.016 (1)
C(1′)A	0.6530 (4)	0.4331 (3)	0.8100 (4)	0.015 (1)
O(1′)A	0.6271 (3)	0.5310 (2)	0.9030 (3)	0.019 (1)
C(2′)A	0.7409 (4)	0.4985 (4)	0.7024 (5)	0.018 (1)
O(2′)A	0.8280 (4)	0.4293 (3)	0.6550 (4)	0.026 (1)
C(3′)A	0.8465 (5)	0.6262 (4)	0.8249 (5)	0.020 (1)
O(3′)A	0.9792 (4)	0.6157 (3)	0.9463 (4)	0.026 (1)
C(4′)A	0.7456 (5)	0.6541 (4)	0.9211 (5)	0.020 (1)
C(5′)A	0.6673 (5)	0.7479 (4)	0.8630 (5)	0.023 (1)
O(5′)A	0.5777 (4)	0.7027 (3)	0.6843 (4)	0.025 (1)
N(11)A	0.7603 (4)	0.0876 (3)	0.6453 (4)	0.018 (1)
C(12)A	0.6379 (5)	0.1333 (4)	0.6011 (5)	0.021 (1)
O(12)A	0.5949 (4)	0.1643 (3)	0.4670 (4)	0.031 (1)
N(13)A	0.5717 (4)	0.1484 (3)	0.7243 (4)	0.016 (1)
C(14)A	0.6311 (4)	0.1163 (3)	0.8782 (4)	0.016 (1)
C(15)A	0.7523 (5)	0.0729 (4)	0.9139 (5)	0.018 (1)
C(16)A	0.8306 (4)	0.0575 (4)	0.7989 (5)	0.017 (1)
O(16)A	0.9450 (3)	0.0262 (3)	0.8218 (4)	0.026 (1)
N(17)A	0.7829 (4)	0.0600 (3)	1.0800 (4)	0.020 (1)
C(18)A	0.6788 (5)	0.0942 (4)	1.1312 (5)	0.021 (1)
N(19)A	0.5810 (4)	0.1288 (3)	1.0099 (4)	0.019 (1)
N(1)B	0.8982 (4)	0.6211 (3)	1.3923 (4)	0.020 (1)
C(2)B	0.7813 (5)	0.5045 (4)	1.3132 (5)	0.022 (1)
O(2)B	0.8105 (4)	0.4056 (3)	1.2911 (4)	0.031 (1)
N(3)B	0.6316 (4)	0.5027 (3)	1.2624 (4)	0.018 (1)
C(4)B	0.6054 (5)	0.6147 (4)	1.2852 (5)	0.018 (1)
C(5)B	0.7203 (4)	0.7322 (4)	1.3605 (4)	0.016 (1)
C(6)B	0.8810 (5)	0.7404 (4)	1.4309 (4)	0.017 (1)
O(6)B	0.9952 (3)	0.8344 (3)	1.5154 (4)	0.022 (1)
N(7)B	0.6542 (4)	0.8264 (3)	1.3630 (4)	0.018 (1)
C(8)B	0.5061 (4)	0.7649 (4)	1.2927 (4)	0.017 (1)
N(9)B	0.4656 (4)	0.6330 (3)	1.2411 (4)	0.017 (1)
C(1′)B	0.3088 (4)	0.5354 (4)	1.1656 (4)	0.017 (1)
O(1′)B	0.3099 (3)	0.4339 (2)	1.2494 (3)	0.0189 (9)
C(2′)B	0.2675 (4)	0.4747 (4)	0.9786 (5)	0.017 (1)
O(2′)B	0.2014 (4)	0.5429 (3)	0.8626 (3)	0.022 (1)
C(3′)B	0.1492 (5)	0.3436 (4)	0.9576 (5)	0.020 (1)
O(3′)B	−0.0023 (4)	0.3463 (3)	0.9308 (4)	0.026 (1)
C(4′)B	0.2081 (5)	0.3124 (4)	1.1311 (5)	0.019 (1)
C(5′)B	0.3033 (5)	0.2261 (4)	1.1371 (5)	0.022 (1)
O(5′)B	0.4212 (4)	0.2788 (3)	1.0725 (4)	0.024 (1)
N(11)B	0.2234 (4)	0.9052 (4)	1.3490 (4)	0.021 (1)
C(12)B	0.3433 (4)	0.8589 (3)	1.3943 (5)	0.016 (1)
O(12)B	0.4076 (3)	0.8524 (3)	1.5390 (3)	0.020 (1)
N(13)B	0.3881 (4)	0.8202 (3)	1.2616 (4)	0.017 (1)
C(14)B	0.3231 (4)	0.8432 (4)	1.1032 (5)	0.016 (1)
C(15)B	0.2080 (4)	0.8964 (4)	1.0692 (5)	0.017 (1)
C(16)B	0.1412 (5)	0.9245 (4)	1.1914 (5)	0.020 (1)
O(16)B	0.0309 (4)	0.9601 (3)	1.1727 (4)	0.035 (1)
N(17)B	0.1700 (4)	0.8992 (3)	0.8990 (4)	0.019 (1)
C(18)B	0.2611 (5)	0.8501 (4)	0.8437 (5)	0.021 (1)
N(19)B	0.3566 (4)	0.8125 (3)	0.9647 (4)	0.019 (1)

At concentrations of 2 ≥ 1 mM voltammetric peak I_a is under linear diffusion control and represents, overall, an irreversible one-electron oxidation reaction.[3] Figure 2 shows a chromatogram of the product solution obtained following an incomplete controlled potential electrooxidation of a saturated solution of **2** at pH 2.0. Chromatographic peak A is due to inorganic phosphate. Chromatographic peaks B and C are due to tertiary alcohols **14** and **15**.[3] The identities of the minor products responsible for chromatographic peaks F and G are not known. Peaks H and I are due to two isomeric compounds having molar masses of 584 g and are therefore dimers of **2** which contain in addition the elements of one molecule of water. Efforts are currently underway to crystallize these compounds in order to employ X-ray diffraction methods to elucidate their structures. Peak X is due to **2**. Peak D is a dimer of **2** which cannot be isolated in a pure form because of its tendency to lose one ribose residue to generate **8**, which is responsible for chromatographic peak E.

Table II. Bond Distances (Å) with esd's in Parentheses

	molecule A	molecule B
N(1)–C(2)	1.383 (4)	1.388 (5)
N(1)–C(6)	1.410 (3)	1.405 (4)
C(2)–O(2)	1.229 (3)	1.234 (4)
C(2)–N(3)	1.365 (5)	1.359 (5)
N(3)–C(4)	1.365 (4)	1.361 (4)
C(4)–C(5)	1.364 (5)	1.376 (5)
C(4)–N(9)	1.368 (5)	1.360 (5)
C(5)–C(6)	1.453 (5)	1.442 (5)
C(5)–N(7)	1.387 (4)	1.386 (4)
C(6)–O(6)	1.215 (5)	1.225 (4)
N(7)–C(8)	1.292 (5)	1.290 (5)
C(8)–N(9)	1.392 (3)	1.399 (4)
C(8)–N(13)	1.414 (4)	1.415 (4)
N(9)–C(1′)	1.463 (5)	1.469 (5)
C(1′)–O(1′)	1.412 (3)	1.409 (3)
C(1′)–C(2′)	1.532 (4)	1.540 (3)
O(1′)–C(4′)	1.465 (4)	1.464 (4)
C(2′)–O(2′)	1.411 (4)	1.423 (3)
C(2′)–C(3′)	1.531 (5)	1.523 (5)
C(3′)–O(3′)	1.415 (5)	1.411 (5)
C(3′)–C(4′)	1.523 (4)	1.527 (4)
C(4′)–C(5′)	1.506 (5)	1.511 (5)
C(5′)–O(5′)	1.441 (4)	1.411 (4)
N(11)–C(12)	1.382 (5)	1.366 (5)
N(11)–C(16)	1.400 (4)	1.406 (4)
C(12)–O(12)	1.213 (3)	1.215 (3)
C(12)–N(13)	1.403 (3)	1.398 (3)
N(13)–C(14)	1.389 (3)	1.385 (3)
C(14)–C(15)	1.353 (5)	1.376 (5)
C(14)–N(19)	1.358 (3)	1.351 (3)
C(15)–C(16)	1.431 (4)	1.432 (4)
C(15)–N(17)	1.384 (3)	1.386 (3)
C(16)–O(16)	1.215 (4)	1.210 (5)
N(17)–C(18)	1.341 (4)	1.332 (4)
C(18)–N(19)	1.341 (4)	1.348 (4)

Crystal Structure of 8. Figure 3[11] is a stereoview of **8**. Molecule A and molecule B are crystallographically independent. The two molecules are related to each other by a pseudocenter of symmetry at approximately (0.5, 0.5, 1.0). Significant deviations from the center of symmetry occur for the sugar moieties of the two molecules in order to accommodate the chiral atom C(1′).

Table II contains bond distances for the two molecules. The two molecules in the unit cell have very similar bond distances except for C(5′)–O(5′), N(11)–C(12), and C(14)–C(15), which show differences larger than 3σ. Bond angles of the two molecules are also comparable except for those on atom N(13). The angle C(8)–N(13)–C(12) differs by 3.1° in molecule A and B and the angle C(8)–N(13)–C(14) by 3.8°. These discrepancies for the two independent molecules are probably due to the different types of hydrogen bonding patterns discussed below.

The imidazole ring in the xanthine group assumes the N(17)–H tautomeric form, established by the location of the N(17) hydrogen atom from the difference Fourier map. One may expect a longer N(17)–C(18) bond than C(18)–

(11) Johnson, C. K. ORTEP, Report ORNL-3794, 1965, Oak Ridge National Laboratory, Tennessee.

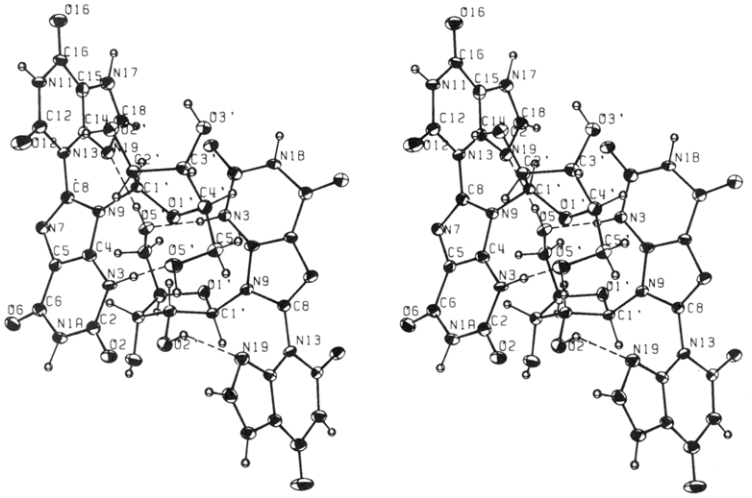

Figure 3. A stereoview of the two molecules A (left) and B (right) of 8 in the unit cell with the atomic numbering scheme, showing also the intramolecular hydrogen bond N(3)–H(3)···O(5′) and the hydrogen bonds in which atom N(19) is involved.

Table III. Hydrogen Bonds in the Crystal Structure

X-H···Y	distances, Å H···Y	distances, Å X–Y	angles, deg X–H–Y
Intramolecular			
N(3)A–H(3)A···O(5′)A	1.74	2.73	170
N(3)B–H(3)B···O(5′)B	1.80	2.67	165
O(2′)A–H(O2′)A···O(12)A	2.46	3.04	134
O(2′)B–H(O2′)B···N(19)B	2.09	2.85	136
Intermolecular			
N(1)A–H(1)A···O(2)B ($x-1, y, z-1$)	1.91	2.82	162
N(1)B–H(1)B···O(2)A ($x+1, y, z+1$)	1.93	2.82	170
O(2′)A–H(O2′)A···O(2)B ($x, y, z-1$)	2.50	3.03	128
O(3′)B–H(O3′)B···O(2′)A ($x-1, y, z$)	2.12	2.83	161
O(3′)A–H(O3′)A···O(2′)B ($x+1, y, z$)	1.91	2.75	157
O(5′)A–H(O5′)A···O(12)B ($x, y, z-1$)	2.04	2.80	159
O(5′)B–H(O5′)B···N(19)A (x, y, z)	1.96	2.71	156
N(11)A–H(11)A···O(6)A ($x+1, y, z$)	2.12	2.95	151
N(11)B–H(11)B···O(6)B ($x-1, y, z$)	2.08	2.93	147
N(17)A–H(17)A···O(16)B ($x+1, y-1, z$)	1.83	2.86	149
N(17)B–H(17)B···O(16)A ($x-1, y+1, z$)	2.02	2.88	157
N(17)A–H(17)A···O(6)A ($x+1, y, z+1$)	2.42	2.97	108
N(17)B–H(17)B···O(6)B ($x-1, y, z-1$)	2.64	3.06	109

N(19). However, the crystal structure shows that the bond distance N(17)–C(18) is equal to C(18)–N(19) for molecule A, and even shorter than C(18)–N(19) by 0.016 Å for molecule B. This may be attributed to the fact that atom N(19) acts as an acceptor in a strong hydrogen bond (see Table III and also Figure 3), leading to a charge delocalization in the imidazole ring. A similar observation was made in the case of anguibactin.[12]

Table III lists all the hydrogen bonds observed in the crystal structure of 3-(8-xanthosyl)xanthine. The bond lengths (H···Y) listed in the table are in agreement with the survey of hydrogen-bond lengths in 75 nucleoside and 11 nucleotide structures.[13] The hydroxyl group O(5′)–H(O5′) acts as the acceptor in an intramolecular hydrogen bond [to N(3)–H(3) in both molecules] and the donor in an intermolecular hydrogen bond [to O(12)B in molecule A and to N(19)A in molecule B]. The O(2′)–H(O2′) group is involved in three hydrogen bonds for molecule A (one intramolecular, two intermolecular), but two for molecule B (one intramolecular, one intermolecular). The atom

(12) Jalal, M. A. F.; Hossain, M. B.; van der Helm, D.; Sanders-Loehr, J.; Actis, L. A.; Crosa, J. H. *J. Am. Chem. Soc.* **1989**, *111*, 292–296.
(13) Jeffrey, G. A. In *Patterson and Pattersons*; Glusker, J. P., Patterson, B. K., Rossi, M., Eds.; Oxford University Press: New York, 1987; pp 193–221.

Table IV. Selected Torsion Angles (deg) with esd's in Parentheses

	molecule A	molecule B	xanthosine[14]
C(8)–N(13) Linkage			
N(7)–C(8)–N(13)–C(12)	90.0 (3)	−78.2 (3)	
N(9)–C(8)–N(13)–C(12)	−81.1 (3)	103.9 (3)	
Glycosyl Bond C(1′)–N(9)			
C(4)–N(9)–C(1′)–O(1′)	36.0 (3)	41.9 (3)	48.9 (3)
C(8)–N(9)–C(1′)–O(1′)	−136.3 (2)	−134.4 (2)	−132.7 (3)
Sugar, Endocyclic			
C(1′)–C(2′)–C(3′)–C(4′)	−34.9 (3)	−33.8 (3)	−34.3 (3)
C(2′)–C(3′)–C(4′)–O(1′)	21.4 (3)	19.5 (3)	20.2 (3)
C(3′)–C(4′)–O(1′)–C(1′)	2.1 (3)	4.1 (3)	3.8 (3)
C(4′)–O(1′)–C(1′)–C(2′)	−25.0 (3)	−25.9 (3)	−26.7 (3)
O(1′)–C(1′)–C(2′)–C(3′)	37.2 (3)	37.3 (3)	38.0 (3)
Orientation of C(5′)–O(5′)			
O(1′)–C(4′)–C(5′)–O(5′)	−64.7 (3)	−65.9 (3)	−65.6 (3)
C(3′)–C(4′)–C(5′)–O(5′)	55.2 (4)	51.7 (4)	54.5 (3)

N(19) bonds to H(O5′)B–O(5′)B for molecule A, but to H(O2′)–B–O(2′)B intramolecularly for molecule B. The atom O(12) bonds to H(O2′)A–O(2′)A intramolecularly for molecule A but to H(O5′)A–O(5′)A for molecule B. The atom O(2)B is the acceptor in two intermolecular hydrogen bonds, while the atom O(2)A is the acceptor in only one intermolecular hydrogen bond. This description shows that the two molecules in the unit cell have different hydrogen bonding patterns. This observation is consistent with the fact that the conformation about the C(8)–N(13) linkage is opposite in the two molecules as indicated by the torsional angle N(7)–C(8)–N(13)–C(12): 90.0° in molecule A and −78.2° in molecule B (Table IV); but on the other hand, the fact that they are opposite reinforces the pseudocentric relationship between molecule A and B.

Table IV gives the selected torsion angles for the two molecules, also compared to those in xanthosine.[14] The conformation about the glycosyl bond, χ_{CN}, ranges for the three molecules from −133° to −136° and is in the syn range. This conformation is stabilized by the intramoleculecular hydrogen bond N(3)–H(3)···O(5′) with the lengths of 2.73, 2.67, and 2.84 Å for molecule A, B (see also Table III), and xanthosine, respectively. The sugar conformation is C(2′)-endo in all three molecules, with torsion angles (see Table IV) resulting in pseudorotation param-

(14) Lesyng, B.; Marck, C.; Saenger, W. *Z. Naturforch. Teil C* **1984**, *39*, 720–724.

Scheme I

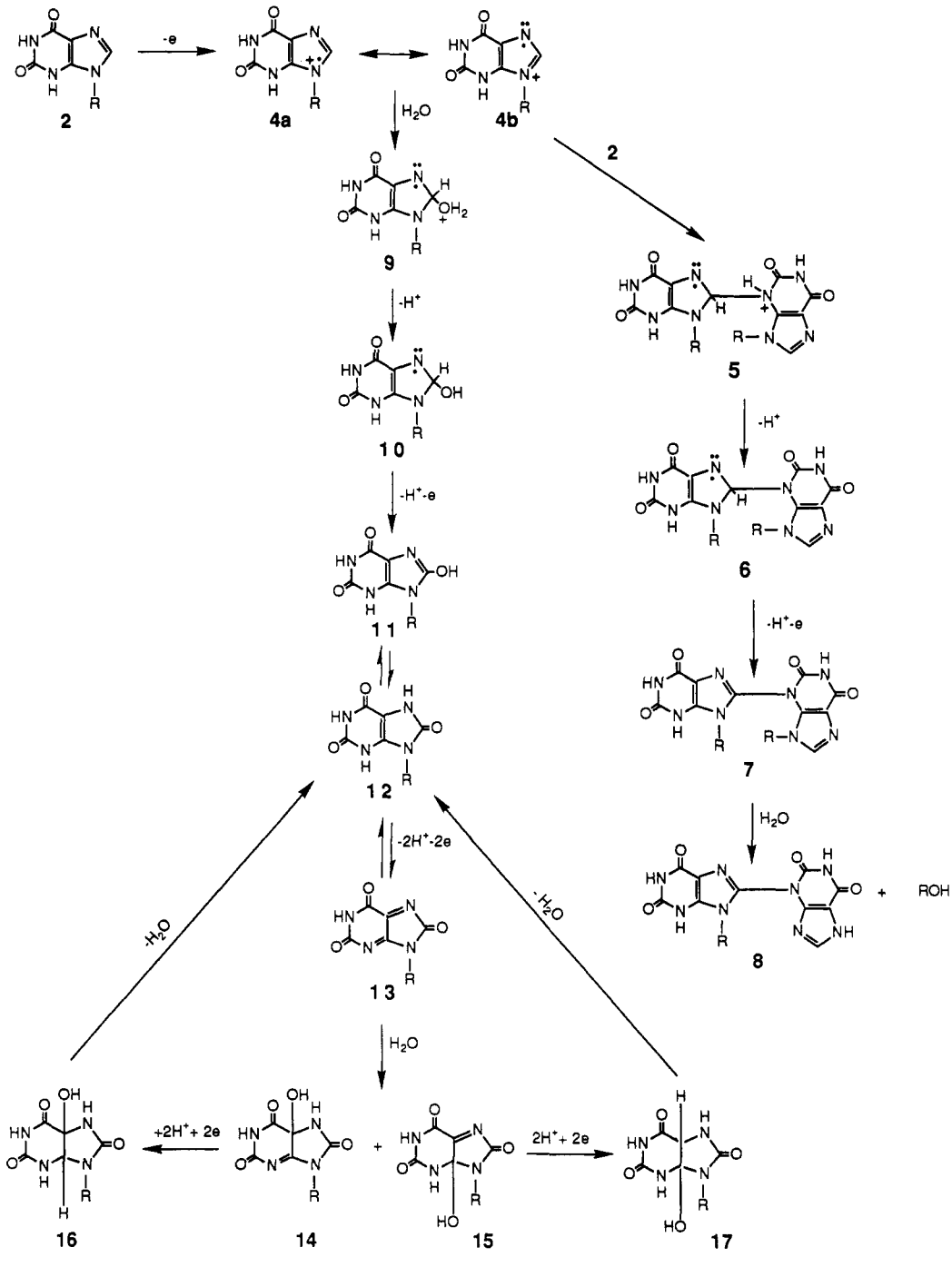

eters (P),[15] which are very similar: 158°, 155° and 156°. The pucker amplitudes (τ_m) are also the same: 37.6°, 37.2°, and 38.7°. The deviations of C(2′) from the plane through the other four sugar ring atoms are 0.582, 0.570, and 0.585 Å for molecule A, B, and xanthosine, respectively. The orientation of C(4′)–C(5′) is gauche–gauche for all three molecules. The unusual intramolecular hydrogen bond O(2′)–H···O(3′) found in xanthosine[14] is, however, not observed in the present compound.

Discussion

Electrochemical oxidation of near-saturated solutions of **2** at low pH generates 3-(8-xanthosyl)xanthosine (**7**) in high yield. However, **7** is not stable in acidic aqueous solution and rapidly loses a ribose unit to form the new dimeric xanthine nucleoside **8**. Compound **7**, however, is stable for a few hours in neutral aqueous solutions. In an earlier report it was speculated that the initial step in the electrochemical oxidation of **2** was a 1e,1H$^+$ reaction to give a C(8)-centered neutral radical, which reacted further to give the ultimate products.[3] Several lines of evidence, however, argue against the intermediacy of such a radical. For example, the most probable product derived from this radical would be **1**. However, no trace of this dimer could be found among the products of electrochemical oxidations of **2**. Furthermore, it is not likely that a neutral C(8)-centered neutral xanthosyl radical species could be converted into 5-hydroxy-$\Delta^{3,4}$-isouric acid (**14**) and 4-hydroxy-$\Delta^{5,7}$-isouric acid (**15**) (see later discussion and ref 3). Clearly, however, formation of **7**, **8**, **12**, **14**, and **15** requires that electrochemical oxidation of **2** activates the

(15) Altona, C.; Sundaralingam, M. *J. Am. Chem. Soc.* **1972**, *94*, 8205–8212.

C(8)-position to nucleophilic attack by water or 2. This might be accomplished by oxidation of 2 to cation 3 as conceptualized in eq 1. Cation 3, however, is undoubtedly

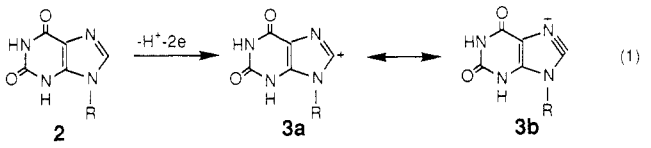

2 3a 3b (1)

a very highly strained compound, and, furthermore, we are unaware of the involvement of such species as intermediates in any similar reactions. Accordingly, we propose that electrochemical oxidation of 2 proceeds by an initial one-electron abstraction reaction to form radical cation 4 (Scheme I). Nadjo and Savéant[16] have theoretically considered the mechanistic pathways by which such an intermediate can be converted to dimeric products in electrochemically driven reactions and have developed diagnostic voltammetric peak characteristics which can be employed to distinguish among these mechanisms. However, only cases where the electron-transfer processes are reversible and diffusion controlled were considered. The experimental peak slope ($E_p - E_{p/2}$ = 80 mV) and pH dependence of the peak potential ($\partial E_p/\partial pH$ = −86 mV)[3] for peak I_a of 2 are greater than expected for a reversible electrode reaction. In addition, adsorption of 2 plays an important role in the peak I_a electrode reaction, particularly at concentrations ≤1 mM, and reactions other than simple dimerization also consume putative radical cation 4. Accordingly, it is only possible to outline a generalized pathway by which 4 is converted to dimer 7. A plausible route involves nucleophilic attack by the most basic nitrogen atom of 2 (pK_a for N(3)–H is 5.67; for N(1)–H is 12.0[17]) on 4 to give the dimer radical cation 5. Deprotonation of 5 would then give neutral radical 6, which is further oxidized (1e,1H$^+$) to 7. The latter oxidation step can in principal be accomplished by a heterogeneous reaction at the electrode surface or by a homogeneous solution electron transfer reaction with 4.[16] Hydrolytic cleavage of one ribose residue yields the structurally characterized nucleoside 8. Nucleophilic attack by water on radical cation 4 would yield radical cation 9, which is further oxidized to 9-β-D-ribofuranosyluric acid (12) by the pathway conceptualized in Scheme I. The latter nucleoside is much more easily oxidized (2e,2H$^+$) than 2 to give quinonoid 13.[18] Attack by water then yields tertiary alcohols 14 and 15. These compounds are not very stable in aqueous solution ($t_{1/2} \approx$ 8–9 min at 25 °C at pH 3[3]) but can be electrochemically reduced at −0.7 V to generate 16 and 17, respectively, which eliminate one molecule of water to form 12.[14] The broad reduction peak at ca. −0.6 V in a CV of 2 (Figure 1) is due to the latter reduction reaction. Peak I_a' is due to the oxidation of 12 formed as a result of this process.[14]

The reaction pathways outlined in Scheme I predict that electrochemical oxidation of high bulk solution concentrations of 2 should produce dimeric products in high yield. With decreasing concentrations of 2, 12 (and hence 14 and 15) should become the predominant products. These predictions are confirmed experimentally. For example, electrochemical oxidation of 2 at concentrations ≤0.1 mM yields 14 and 15 as the major initial products along with only traces of dimeric products.[3] On the other hand, oxidation of near-saturated solutions of 2 yields dimers as the major products.

Conclusions

This study establishes the molecular structure of the new dimeric nucleoside of xanthosine 8 formed as a result of the electrochemical oxidation of 2 in aqueous solution. The key intermediate in the electrode reaction is proposed to be radical cation 4, which is susceptible to nucleophilic attack by 2 in a reaction sequence that leads to 3-(8-xanthosyl)xanthosine (7). One ribose residue is hydrolytically cleaved from 7 to yield 8. Several years ago Hatfield and Wyngaarden[19] showed that 3-ribosylxanthine-5′-phosphate is produced in the reaction of xanthine with pyrophosphorylribose phosphate and the enzyme pyrimidine ribonucleotide pyrophosphorylase isolated from bovine erythrocytes. It is interesting to speculate whether a radical cation intermediate might be involved in the formation of the N(3)–C bond formed in this unusual xanthine nucleotide. It is also of interest to note that 8 has several structural features in common with the most specific adenosine antagonist in the central nervous system 8-phenyl-1,3-dimethylxanthine.[20]

Acknowledgment. This work was supported in part by Grant no. GM-21034 from the National Institutes of Health and Grant no. CA 17562 from the National Cancer Institute. Additional support was provided by the Research Council of the University of Oklahoma.

Registry No. 2, 146-80-5; 7, 124419-29-0; 8, 124419-28-9.

Supplementary Material Available: Tables of bond angles, anisotropic thermal parameters for non-hydrogen atoms, fractional coordinates, and isotropic thermal parameters for hydrogen atoms (5 pages); structure factor tables (18 pages). Ordering information is given on any current masthead page.

(16) Nadjo, L.; Savéant, J. M. *J. Electroanal. Chem. Interfacial Electrochem.* **1973**, *44*, 327–366.
(17) Zorback, W. W., Tipson, R. S., Eds.; *Synthetic Procedures in Nucleic Acid Chemistry*; Wiley-Interscience: London, 1973; p 496.
(18) Tyagi, S. K.; Dryhurst, G. *J. Electroanal. Chem. Interfacial Electrochem.* **1987**, *223*, 119–141.
(19) Hatfield, D.; Wyngaarden, J. B. *J. Biol. Chem.* **1964**, *239*, 2580–2586, 2587–2592.
(20) Smellie, F. W.; Davis, C. V.; Daly, J. W.; Wells, J. N. *Life Sci.* **1979**, *24*, 2475–2482.